

## \* Increasing Stability of Biotin Functionalized Electrospun Fibers for Biosensor Applications

\* Increasing Stability of Biotin Functionalized Electrospun Fibers for Biosensor Applications

Larissa M. Shepherd<sup>1</sup>, Edurne Gonzalez<sup>1</sup>, Esther Chen<sup>2</sup>, Margaret W. Frey<sup>1\*</sup>

<sup>1</sup> Department of Fiber Science & Apparel Design, Cornell University, Ithaca, New York;  
E-mail(s): [lb468@cornell.edu](mailto:lb468@cornell.edu) (L.S.), [eg452@cornell.edu](mailto:eg452@cornell.edu) (E.G)

<sup>2</sup> Department Biomedical Engineering, Cornell University, Ithaca, New York;  
E-mail(s): [ec685@cornell.edu](mailto:ec685@cornell.edu) (E.C.)

\* Author to whom correspondence should be addressed; E-mail: [margaret.frey@cornell.edu](mailto:margaret.frey@cornell.edu) (M.F.);  
Tel.: +1-607-255-1937; Fax: +1-607-255-1093.

*Received: / Accepted: /Published:*

---

### Abstract

This paper describes the effects of both solvent and altering the block lengths of PLA-b-PEG on water stability of electrospun PLA/PLA-b-PEG and PLA/PLA-b-PEG-Biotin fibers. By tailoring the block length of copolymers PLA-b-PEG, water stability of electrospun fibers is improved over fibers formed previously. Studying solvents DMF and HFIP revealed that fibers formed using HFIP have greater water stability, but less PEG at surface of fibers than DMF spun fibers. Attaching biotin to the end of PLA(3600)-b-PEG(2000) and spinning from DMF allowed for 1.1 mg of biotin per gram of fiber to be detected at the surface of fibers, that is 7.6 % of the total biotin incorporated into the fiber (assuming every PEG terminal has one biotin attached). In addition, PLA/PLA(3600)-b-PEG(2000)-Biotin spun from DMF hindered biotin migration to the aqueous phase, with 2 % of biotin remaining at the surface of fibers after seven days of water exposure. By attaching biotin directly to the copolymer, as opposed to adding biotin freely to the dope, this study was able to add 85 % less biotin and still achieve the same relative amount of biotin available at the surface of fibers for chemical detection. While HFIP spun fibers lost little biotin, its use resulted in biotin being at the interior of the fibers, showing little to no surface available biotin.

**Keywords:** electrospinning; block length; biotin

---

## 1. Introduction

Nanofiber membranes have very high surface area to volume ratios and porous structures, making them excellent candidates for chemical detection and biosensor applications [1-4]. A nanofiber mat's ability to be implemented as a biosensor, however, is limited by the ability to control several polymer characteristics that include: (i) hydrophobic polymers that limit its use in aqueous biological systems, (ii) hydrophilic polymers solubility in aqueous media, and (iii) fiber surface functionality.

One method researchers use to tailor fiber and membrane properties is incorporating polymeric and oligomeric materials directly to the processing dopes. For example, the blending of a hydrophobic polymer and a hydrophilic additive may yield a less hydrophobic membrane.[5-7] For example, using a modified electrospinning system with poly(lactic acid) (PLA)/PLA-b-poly(ethylene glycol) (PLA-b-PEG) Buttaro et al. found phase separation of PEG to surface of the fibers resulting in a hydrophilic polymer.[8] We build on this work in order to increase the surface functionality of fibers.

Biotin finds common use in biosensor applications based on rapid protein binding and a wide variety of functionalized chemistries available for specific biomolecule capture. [4, 9-11] By functionalizing PLA nanofibers with biotin, there is a high surface area to volume ratio that can be used for sensitive chemical detection in aqueous media. Li. et al. attempted to address the functionality of the fiber and was able to show that biotin was present at the surface of PLA fibers, but the hydrophobic nature of PLA and the long term stability under aqueous conditions of biotin in the fiber was not investigated.[9] Using PLA/PLA-b-PEG, Gonzalez et al. was able to significantly increase the amount of available biotin at the surface of PLA fibers, as the PLA-b-PEG aided in the migration of biotin to the surface of the fibers. While the biotin at the surface increases, after 24 hours of water exposure the hydrophilic biotin preferentially diffuses into the surrounding water. The copolymer then also diffuses into the water, further reducing the fiber scaffolds' functionality significantly, after seven days of exposure.[12]

By binding biotin directly to PLA-b-PEG and optimizing the block copolymer, water solubility of biotin and the block copolymer can be minimized. Functionalization of biotin at the fiber's

surface with antibodies is the next step for using this nanofiber system as a sensor. Antibodies, however, are sensitive to denaturing with heat and exposure to organic solvents. The main solvent we have used to investigate biotin functionalized fibers is DMF, which is both an organic solvent and requires heating prior to and during electrospinning; if antibodies were to be added directly to this dope denaturing is probable. Nuansing et al. electrospun pure protein from the fluorinated solvent HFIP and found little to no denaturation of the protein.[13] Therefore, in an effort to overcome potential denaturing in the future, this study will also investigate and compare the surface available biotin present when we use solvents DMF as well as HFIP.

If biotin functionalized PLA/PLA-b-PEG fibers are to be useful as sensors in aqueous environments for long duration, we must address the water stability of PLA/PLA-b-PEG fibers by finding appropriate block lengths of PLA-b-PEG. In this paper, we investigate the use of copolymer block length to increase the stability of PLA-b-PEG-Biotin nanofiber membranes while maintaining surface functionality. We also analyze the effect of solvent and polymer concentration in the final fiber on stability and surface available biotin.

## **2. Experimental**

### *2.1. Materials*

PLA-b-PEG block copolymers were synthesized by ring opening polymerization of lactide (Sigma-Aldrich) in the presence of poly(ethylene glycol) methyl ether (Number average molecular weights (Mn) : 1000 g/mol, (Mn) : 2000 g/mol, and (Mn) : 5000 g/mol using catalyst stannous octate (Sigma- Aldrich). The copolymers produced were PLA(5000)-b-PEG(1000), PLA(2800)-b-PEG(2000) and PLA(5300)-b-PEG(5000). To produced biotin functionalized polymer PLA(3600)-b-PEG(2000)-Biotin and PLA(5700)-b-PEG(1000)-Biotin, biotin-poly(ethylene glycol) methyl ether with PEG block lengths (1000) and (2000) were purchased from Creative PEGWorks. PLA 4043D (MW= 153,315g/mol, PDI=1.81) was purchased from NatureWorks LLC(Minnetonka, MN). Solvents 1,1,1,3,3,3-Hexafluoro-2-propanol and 99.8 % anhydrous N,N-Dimethylformamide(DMF), were purchased from Sigma-Aldrich (St. Louis, MO). 25-gauge x 1 needles were purchased from (Small Part Inc.) and needle deflect point 20-gauge x 2inch were purchased from Fisher Scientific Company LLC (Suwanee, GA). For colorimetric assays we used Pierce™ biotin quantification kits purchased from ThermoScientific.

## 2.2. Electrospinning

All spinning dopes in this study are made of high molecular weight PLA and PLA-b-PEG copolymers. The amount of block copolymer was adjusted to obtain 12 wt% or 26 wt% of PEG in the final fibers. All DMF solutions had 12 wt% PEG, as previous work showed that the greatest water wicking occurred at this concentration. [8] For comparison, we also investigated 12 wt% PEG with HFIP. After characterization of the block lengths of PLA-b-PEG (Figure 1A) that promote the greatest water wicking and demonstrate excellent water stability, we synthesized PLA-b-PEG with biotin at the other terminal end of the PEG blocks (Figure 1B). The maximum biotin loading was limited by the PLA-b-PEG block length as the PEG loadings were fixed throughout these studies.

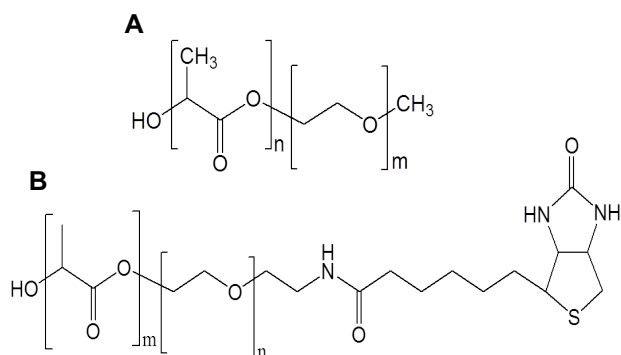


**Figure 1.** Molecular structures of polymers synthesized by solution polymerization (A) PLA-b-PEG, and (B) PLA-b-PEG-Biotin.

Using HFIP as the solvent for PLA in the electrospinning dope resulted in the formation of a suspension when we added PLA-b-PEG or PLA-b-PEG-Biotin (note PLA is completely soluble in HFIP). This suspension does settle over time, so we agitated them prior to use. The spinning dopes contained 3.6 wt% PLA (high molecular weight homopolymer) and were placed on a wrist shaker for at least 16 hours prior to electrospinning to form the spinning dopes. We used a standard electrospinning system at a feed rate of 1.5mL/hr (PHS Ultra syringe pump, Harvard Apparatus) to form fibers from the PLA-b-PEG and PLA-b-PEG-Biotin suspensions. We drove fiber formation by applying 15 kV (Gamma High Voltage Research Inc., FL) between a 25 g needle tip and grounded collector consisting a copper sheet wrapped in aluminum ~ 22cm way ( $68 \text{ kV m}^{-1}$  gradient field).

For comparison, we also used DMF as a solvent because, with heating, it can dissolve more PLA and copolymers of PLA (22 wt%)[8, 12] without forming a suspension. We used a modified electrospinning apparatus[8] to keep the syringe at  $70^{\circ}\text{C} \pm 5^{\circ}\text{C}$  and applied a field 15 kV(Gamma High Voltage Research Inc., FL) between the metal needle and the grounded collector (copper sheet wrapped in aluminum) placed  $\sim 10$  cm away ( $150\text{ kV m}^{-1}$  gradient field). We maintained a solution feed rate of  $10\ \mu\text{L}/\text{min}$  using a programmable PHS Ultra syringe pump (Harvard Apparatus).

We stored all samples in a desiccator prior to water wicking, stability, DSC, and SEM studies. PLA fibers spun from DMF was done previously and stored at room temperature prior to experiments.

### *2.3. Water Stability*

To study the stability of the nanofiber membranes in water, we cut  $\sim 4 \times 1/2$  cm rectangles (in excess of 0.0099 g) of the deposited mats. Cut samples were placed in 15mL of DI water for either 24 hrs or 7 days. After we removed them from the DI water, we placed them in a vacuum oven set to  $25^{\circ}\text{C}$  (oven temperature ranged from  $24$  to  $29^{\circ}\text{C}$ ) for 24 hrs. Note that fiber mate samples of PLA/PLA(5700)-b-PEG(1000)-Biotin shrunk a couple of centimeters prior to experiments.

### *2.4. Nuclear Magnetic Resonance Spectroscopy (NMR)*

We analyzed the NMR spectra on the control and dried samples to more accurately measure copolymer dissolution.  $^1\text{H-NMR}$  experiments were recorded at room temperature with an INOVA 400 spectrometer (Varian Inc., Palo Alto, CA, USA) operating at 400 MHz. Deuterated chloroform ( $\text{CDCl}_3$ ) was used as solvent and tetramethylsilane (TMS) as an internal reference.

### *2.5. Differential Scanning Calorimetry (DSC)*

Using a DSC Q2000, we determined the effects of PEG on the overall fiber properties. Our samples are heated cyclically from  $-80^{\circ}\text{C}$  to  $180^{\circ}\text{C}$  at a rate of  $5^{\circ}\text{C}/\text{min}$ , cooled to  $-80^{\circ}\text{C}$  at a rate of  $2^{\circ}\text{C}/\text{min}$ , and re-heated at a rate of  $5^{\circ}\text{C}/\text{min}$  to investigate whether or not PEG phase separates and if PLA's crystallization is induced by electrospinning and solvent effects. Control

PLA samples spun from DMF were done previously and only investigated cyclically from 5°C to 180°C at a rate of 5 °C/min, cooled to 5°C at a rate of 2 °C/min, and re-heated at a rate of 5 °C/min.

## 2.6. Field Emission Scanning Electron Microscopy (FE-SEM)

By using an FE-SEM, we observed the microstructure of the fiber mats in high contrast. We sputter coat samples in gold-palladium for 30s prior to imaging them with a LEO 1550 FESEM using a 1kV accelerating voltage and 50:50 mixture of SE2 and InLens detectors. Using ImageJ™ software on the recorded SEM images, we calculated the average diameters from 50 fiber measurements gathered from two images.

## 2.7. Water Wicking

Each electrospun sample was cut into 3 x ½ cm fabrics. We weighed the samples and then put a fishhook through the nanofabric to ensure the membrane penetrated the meniscus.[8] Wettability testing was done using the KSV Sigma 701 and DI water. Note that fiber mat samples of PLA/PLA(5700)-b-PEG(1000)-Biotin shrunk a couple of centimeters prior to experiments.

## 2.8. Biotin/Avidin Binding

We are able to compare the effect of solvent on biotin reaching the fiber surface by using a quantifiable competitive colorimetric assay, whose change in absorbance at 500nm signifies the avidin removal from a 4'-hydroxyazobenzene-2-carboxylic acid (HABA)/Avidin solution to the fiber surface containing biotin. A Lambda 35 UV/Vis spectrophotometer from Perkin Elmer is used to measure the change in absorbance. We reconstituted HABA/Avidin solutions by the manufacturer's protocol, and took it's absorbance in PBS Buffer at 500nm. We weighed the nanofiber fabrics prior to placing them into a cuvette and shaking for three minutes; afterwards, we removed the fiber mat and measured the absorbance. Equation 1 is used to calculate the available biotin at the surface of fibers.[12] For each sample we perform at least three replicates.

$$[biotin] = (A_{500}^0 - A_{500}) \left( \frac{Mw_{biotin}V}{\epsilon bW} \right) \quad \text{Equation 1}$$

Where  $A_{500}^0$  is the absorbance of the solution prior to the addition of nanofiber,  $A_{500}$  is the absorbance of the solution after reaction with nanofiber,  $MW_{biotin}$  is the molecular weight of the biotin (244.3 g/mol),  $V$  is the volume of the solution (L),  $b$  is the cuvette path length (1 cm) and  $\epsilon$  is the extinction coefficient of the HABA/Avidin complex at 500 nm ( $3.4 \times 10^{10}$  L/(mol cm)).

### 3. Results and discussion

#### 3.1. PLA/PLA-*b*-PEG Fiber Stability in Water

Changing PLA and PEG block lengths and electrospinning solvent both significantly impacted the stability of the resulting electrospun fiber mats in water (Figure 2). While it was possible to form good nanofibers containing 26 wt% PEG from PLA(5300)-*b*-PEG(5000) using HFIP as the solvent, stability of these fibers in water was very poor with a 35 % loss of copolymer by NMR after seven days (Figure 2). Fibers containing 26 wt% PEG from PLA/PLA(2800)-*b*-PEG(2000) spun from HFIP produced insufficient nanofibers and lost ~ 50 % of copolymer after seven days of water exposure. Therefore, aside from DSC studies, the remainder of this article we will focus on fibers containing 12 wt% PEG.

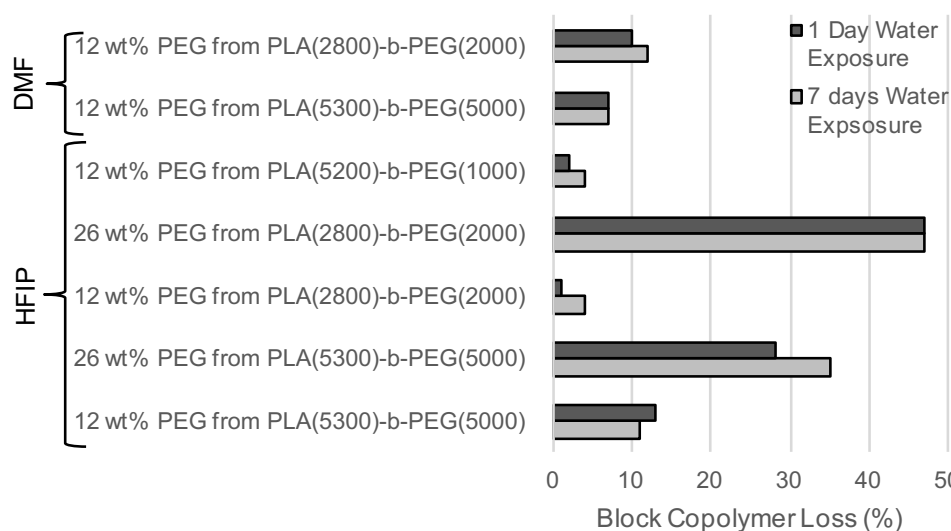


**Figure 2.** Block copolymer weight loss after one day and seven days of water exposure as determined by NMR.

Electrospun fibers containing 12 wt% PEG from PLA(5300)-*b*-PEG(5000), and PLA(2800)-*b*-PEG(2000) spun from DMF and HFIP were studied for copolymer loss by a change of composition in NMR spectra (Figure 2). As reported previously, solutions with 12 wt% PEG

from PLA(5200)-b-PEG(1000) in DMF were not spinnable, [8] however fibers could be formed and studied for copolymer loss when spun from HFIP (Figure 2). Considering just copolymers spun from DMF, by only altering the block lengths, we are able to significantly decrease the loss of copolymer from 64 % for PLA(730)-b-PEG(5000) reported by Gonzalez et al.[12] to less than 10 % after seven days of water exposure. We further increased the stability of the copolymer when we used HFIP as the electrospinning solvent.

Interestingly, block copolymer stability within fibers spun from DMF slightly improves for longer block lengths of PEG, whereas fibers spun from HFIP are more stable with shorter PEG block lengths (at 12 wt% PEG fiber loadings). By changing the solvent of the spinning dopes from DMF to HFIP, over seven days of water exposure we decreased the copolymer loss of PLA(2800)-b-PEG(2000) (for 12 wt% PEG in the final fiber) from 12 % to 4 %. Differences in both the spinning dopes and the resulting fiber morphologies contribute to the difference observed in water stability. The HFIP spinning dope is spun from a suspension that is likely to contain micelles and their aggregates and not a homogenous like the DMF dope. We imaged an HFIP solution with copolymer that has settled (Supplemental Figure S1) and therefore assume micelle aggregates have formed as the PLA is soluble in HFIP, but under the conditions of this study the PEG was not. Further analysis presented below details the differences in the PEG phase formation within the fiber and fiber structure.

### 3.2. PLA/PLA-b-PEG Fiber Thermal Behavior

We gather thermal processing information based on the first heating of cyclical thermographs. In order to compare the crystallization of PLA with the addition of block copolymers, we use Equation 2, where  $X_c$  is the % crystallinity,  $\Delta H_c$  is the heat of cold crystallization ( $J \cdot g^{-1}$ ),  $\Delta H_f$  is the heat of fusion ( $J \cdot g^{-1}$ ), and  $\Delta H_{m^o}$  is the heat of fusion for 100 % crystalline PLA (here we use  $93.6 J \cdot g^{-1}$  [14]). We correct for samples containing PEG by dividing by the fraction of PLA in the final fibers (0.88 for 12 wt% PEG fibers and 0.74 for 26 wt% PEG fibers).

$$X_c = \frac{\Delta H_f - \Delta H_c}{\Delta H_{m^o}} \times 100$$

Equation 2



We find PLA-PEG more effectively crystallizes PLA when spun from DMF; whereas, when spun from HFIP, PLA crystallization was hindered when PLA(5200)-b-PEG(1000) was added and not significantly changed at larger PEG block lengths (Figure 3A). As mentioned previously, when polymers are spun from HFIP, there are likely micelle aggregates that have formed as the result of PEG insolubility in HFIP, thereby reducing PEG's effectiveness in plasticizing PLA (Figure 3B). There is a slight decrease in PLA's crystallinity when the copolymers were spun at 26 wt% PEG, however this may can be considered as sample to sample variation. Due to the ratio of PLA:PEG in copolymer PLA(5200)-b-PEG(1000), we were unable to produce dopes/fibers using HFIP at 26 wt% PEG, therefore there is no value represented here.

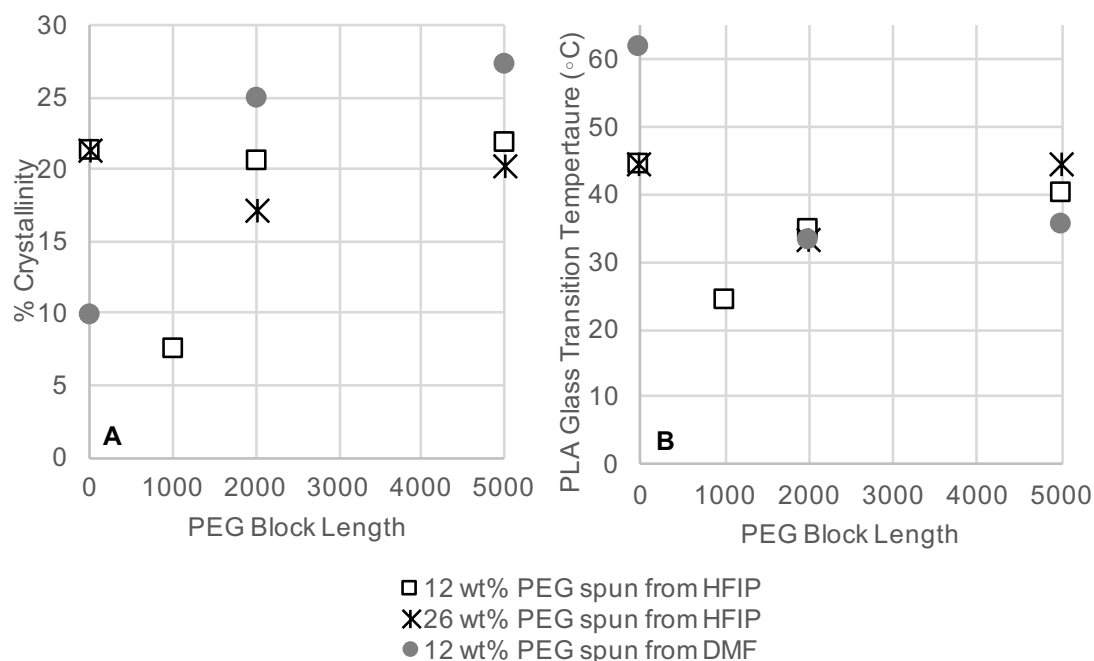


**Figure 3.** DSC data. (A) Percent crystallinity of PLA in electrospun fibers in relation to block length PEG and solvent (B) Glass transition temperature of PLA compared to PEG block length and solvent.

HFIP spun fibers exhibit a similar trend between the amount of PLA crystallinity and the glass transition temperature of PLA ( $T_g^{PLA}$ ), while the DMF spun samples display an opposing trend (Figure 3). DMF samples, which are spun at elevated temperatures, are produced from a more concentrated homopolymer PLA solution than that of HFIP fibers, meaning that DMF dopes are more frustrated systems. [15, 16] While frustrated systems want to be crystalline, they do not

have as much mobility as a more dilute solution would to reorganize into its crystalline form. Therefore, when no copolymers are added, DMF solutions have a lower crystallinity but a higher  $T_g^{PLA}$  than PLA spun from HFIP. Interestingly, HFIP fibers have a decrease in crystallinity and  $T_g^{PLA}$  (Figure 2B) when 12 wt% of PLA5200-b-PEG (1000) is incorporated into the fibers. This drop can be associated with the greater plasticizing effect of the shorter block length of PEG.

When looking at the copolymer fibers electrospun from DMF and HFIP we find distinct differences on the second heating of the fibers (Figure S2). First, polymers spun from HFIP, with the exception of PLA(5200)-PGE(1000), do not display the two crystalline forms  $\alpha'$  and  $\alpha$  phase transition of PLA but rather hinder this transition, which the fibers spun from DMF promote; this  $\alpha'$  to  $\alpha$  phase transition is the polymer going from a less ordered crystal to a more ordered one. [17] In addition, when spun from DMF, there is no longer a cold crystallization peak for PLA whereas when spun from HFIP, while small, it still exists. These disparities in cyclic heating show differences between the solvents used to electrospin fibers and ultimately how PEG is affecting the final fibers' properties.

### 3.3. PLA/PLA-b-PEG Fiber Morphology

Compared to pure PLA fibers, fibers spun from DMF decrease in fiber diameter when copolymers are added to the dope, however, fibers spun from HFIP increase in fiber diameter when copolymers are added. HFIP and DMF spun fibers both increase in fiber diameter for increasing PEG block length (Figure 4). HFIP fibers containing PLA(5200)-b-PEG(1000) have the largest diameter; this increase is associated with the melding of fibers as a result of landing wet with residual solvent. Since fibers land wet, they take on a ribbon shape rather than a circular or oval shape. As a result, when we measure fiber diameters, larger diameters are observed. While the cross section perpendicular to the fiber's axis has a larger diameter, the cross section along the fiber axis would have a much smaller diameter since it is not round. In addition, the copolymers themselves differed in texture, which may have further contributed to this observance; the higher molecular weight copolymers form powders while the lower molecular weights form a tacky viscous substance (Figure S3).

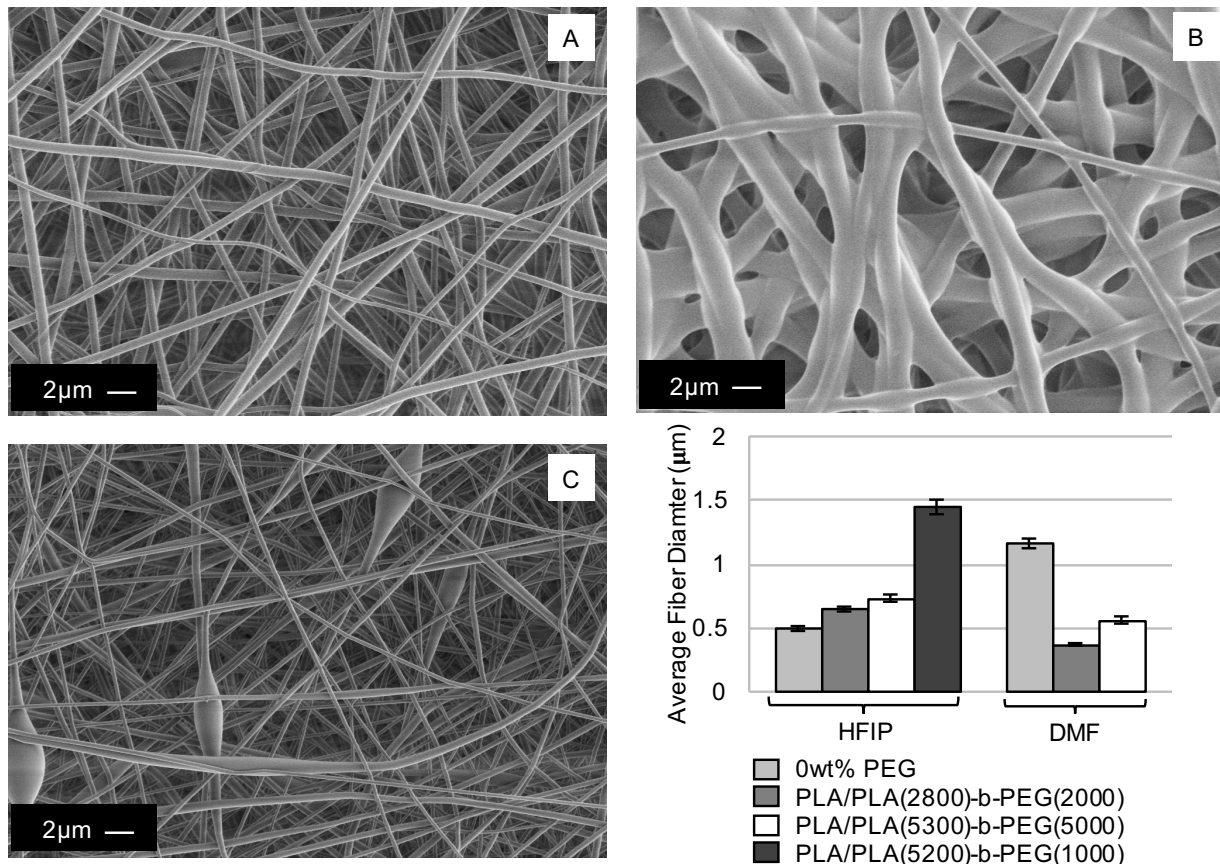


**Figure 4.** SEM images of (A) 12 wt% PEG from PLA(2800)-b-PEG(2000) spun from HFIP, (B) 12 wt% PEG from PLA(5200)-b-PEG(1000) spun from HFIP, and (C) 12 wt% PEG from PLA(2800)-b-PEG(2000) spun from DMF. Average fiber diameters are represented in the graph for control PLA fibers and fibers containing 12 wt% PEG from PLA-b-PEG copolymers. Error bars represent standard error.

### 3.4. PLA/PLA-b-PEG Fiber Water Wicking

Fibers containing copolymers with PEG block lengths of 2,000 and 5,000 do not wick as much water per their weight when spun from HFIP as compared to DMF spun samples (Figure 5). This indicates DMF promotes PEG to the fiber surface more effectively than HFIP. DMF samples spun from PLA/PLA(5300)-b-PEG(5000) wicked approximately 1,100 % its own fiber weight in water. Fibers of PLA/PLA(1000)-b-PEG(2000) spun from DMF were also able to wick a similar amount. Interestingly, fibers of PLA/PLA(5200)-b-PEG(1000) spun from HFIP had an increase in water wicking, which is associated with the flat ribbon-like fiber morphology previously mentioned.

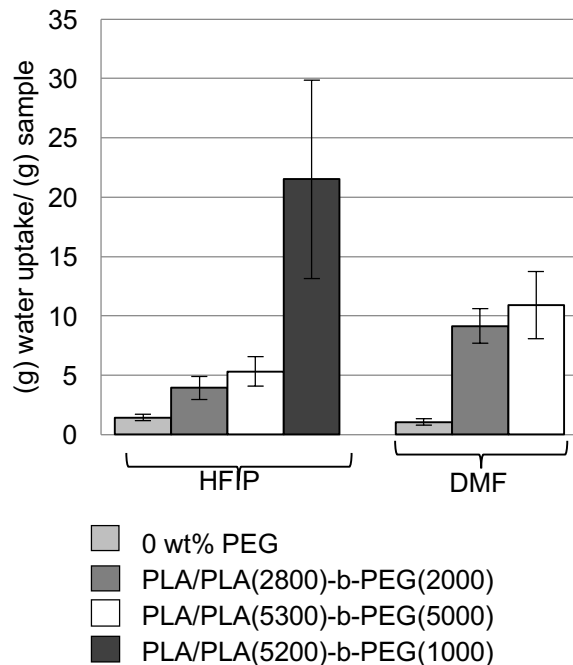


**Figure 5.** Water wicking data for control PLA fibers and fibers containing 12 wt% PEG from PLA-b-PEG. Error bars represent standard error.

We considered the amount of copolymer lost and water wicking data of the fiber mats to be the determining parameters in what copolymers to synthesize with biotin attached. For this reason, we synthesized PLA(5700)-b-PEG(1000)-Biotin. As mentioned earlier PLA(5200)-b-PEG(1000) was not able to be spun from DMF, for this reason we also synthesized PLA(3600)-b-PEG(2000)-Biotin. We extensively study both copolymers in the following sections.

### 3.5. PLA/PLA-b-PEG-Biotin Fiber Stability in Water

We use NMR to determine copolymer lost after 1 and 7 days of water exposure for fibers spun from HFIP and DMF (Figure 6). As with the polymers synthesized without biotin attached, we observe some loss of PLA-b-PEG-Biotin copolymers with exposure to water. The fiber spun from DMF lost the most PLA-b-PEG-Biotin, up to 16 % of the total copolymer put into the fiber after 7 days. This loss is the result of the phase separated copolymer being present at the surface of fibers and preferentially migrating to the aqueous media. Fibers spun from HFIP lost far less PLA-b-PEG-Biotin compared to the DMF spun fiber, which was also previously shown in our study of PLA/PLA-b-PEG spun fibers.

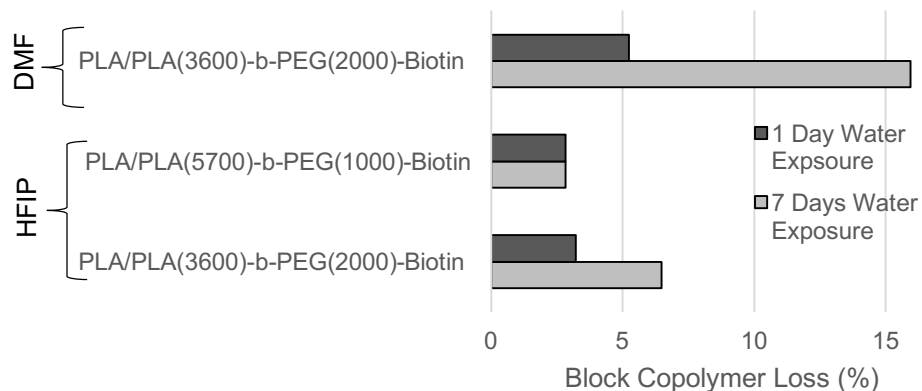


**Figure 6.** PLA-b-PEG-Biotin weight loss after one day and seven days of water exposure as determined by NMR.

### 3.6. PLA/PLA-b-PEG-Biotin Fiber Morphology

To be complete, we again look at fiber morphology and diameter size (Figure 7). With the exception of PLA/PLA(5700)-b-PEG(1000)-Biotin, fiber diameter decreases when biotin is attached. When PLA/PLA(5700)-b-PEG(1000)-Biotin is spun from HFIP, the fibers take on a larger diameter and a more spherical shape as compared to when biotin was not attached to the copolymer (PLA(5200)-b-PEG(1000)). This change in morphology is a function of both biotin being attached and, more importantly, because the PLA block length is slightly longer, we no longer have flattening of the fibers by residual solvent.

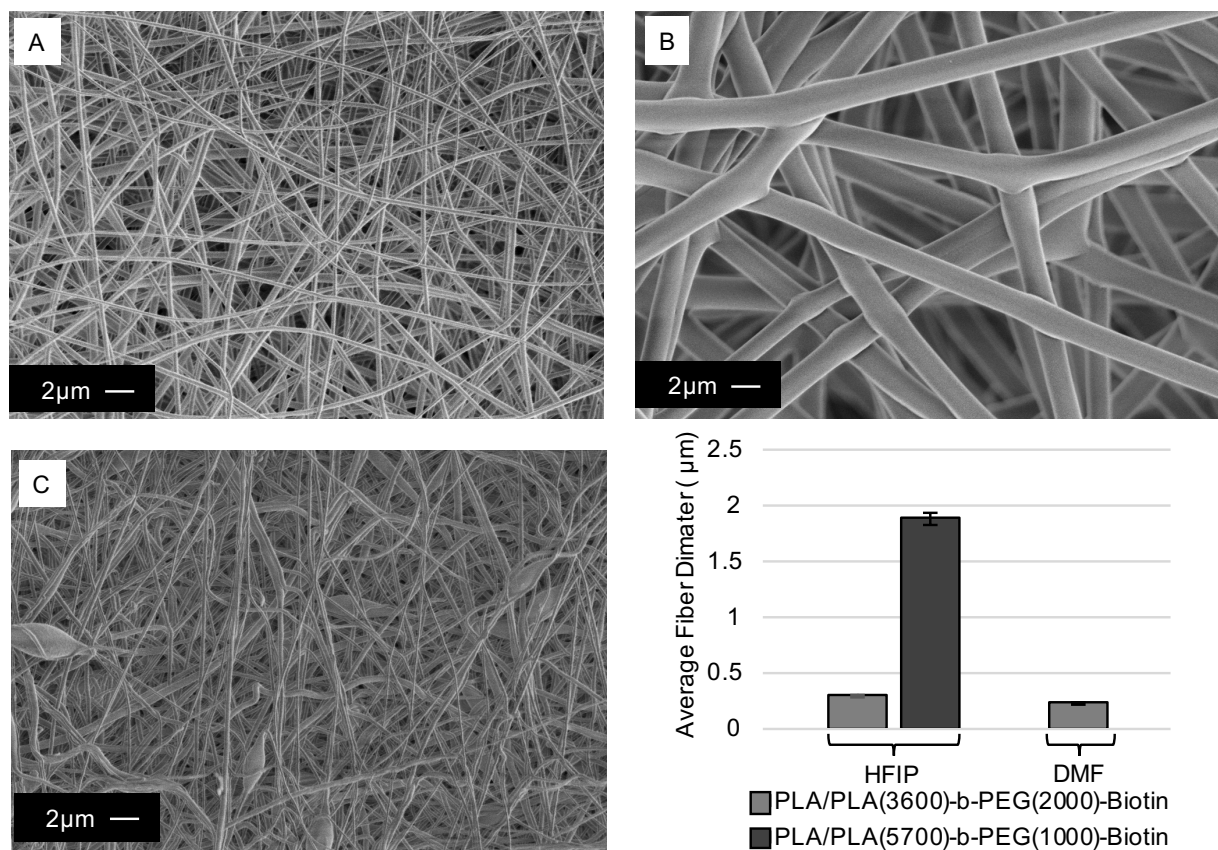


**Figure 7.** SEM images of (A) 12 wt% PEG from PLA(3500)-b-PEG(2000)-Biotin spun from HFIP, (B) 12 wt% PEG from PLA(5700)-b-PEG(1000)-Biotin spun from HFIP, and (C) 12 wt% PEG from PLA(3600)-b-PEG(2000)-Biotin spun from DMF. Average fiber diameters are represented in the graph for fibers containing 12 wt% PEG from PLA-b-PEG-Biotin. Error bars represent standard error.

### 3.7. PLA/PLA-b-PEG-Biotin Fiber Water Wicking

While the fibers spun from HFIP lost less copolymer, the low water wicking provides evidence of smaller quantities of PEG and biotin present at a fiber's surface compared to fibers spun from DMF (Figure 8). Interestingly, the hydrophilic nature of the fibers spun from DMF increases with the incorporation of biotin, while the fibers spun from HFIP remain relatively unchanged or decrease in hydrophilicity. The fibers spun from HFIP containing PLA(5700)-b-PEG(1000)-Biotin show a drastic loss in hydrophilicity compared to when the copolymer PLA(5200)-b-PEG(1000) was electrospun. This change is explained by fiber diameter being larger and the

circular morphology, rather than ribbon shaped and oval. As a result of the water wicking data, DMF electrospun samples would be more useful as biosensors in aqueous environments than the less hydrophilic samples spun using HFIP.

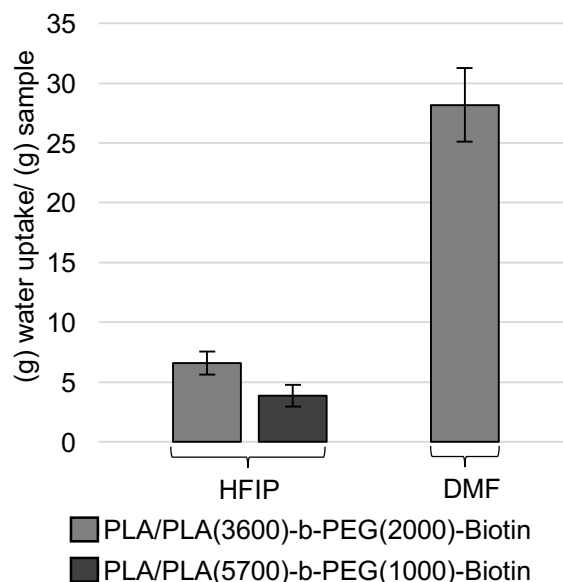


**Figure 8.** Water wicking data for fibers containing 12 wt% PEG from PLA-b-PEG-Biotin. Error bars represent standard error.

### 3.8. PLA/PLA-b-PEG-Biotin Surface Available Biotin

The available biotin at the fiber's surface is significantly impacted by the solvent system used. The use of HFIP dopes with either PLA(3600)-b-PEG(2000)-Biotin or PLA(5700)-b-PEG(1000)-Biotin have little to no biotin at the surface of fibers (Figure 9), and with exposure to DI water for one and seven days there is virtually no increase in biotin at the surface. This is again explained by the insolubility of PEG in HFIP that is likely producing micelle aggregates in the spinning dopes which is preventing the phase separation of PEG-Biotin to the fiber's surface. On the contrary, with dopes of DMF where phase separation is known to be aided by the modified electrospinning process used in this study[8], we are able to increase the amount of surface available biotin to a far greater degree than when Li et al. added biotin freely to the electrospinning dope. With ~15 mg of biotin per gram of fiber, we detect on average 7.6 % of available biotin at the surface of the fibers (assuming every PEG has one biotin attached), resulting in 1.1 mg of biotin per gram of fiber (Figure 9); Li et al. who incorporated 10 wt% biotin (100 mg of biotin per gram of fiber) was only able to detect 1.2 mg of biotin per gram of

fiber, resulting in detection of only 1.2 % of the biotin incorporated into the fiber. Consequently, by attaching biotin directly to the copolymers we are able to add 85 % less biotin, but still achieve the same relative amount of biotin at the fiber's surface.

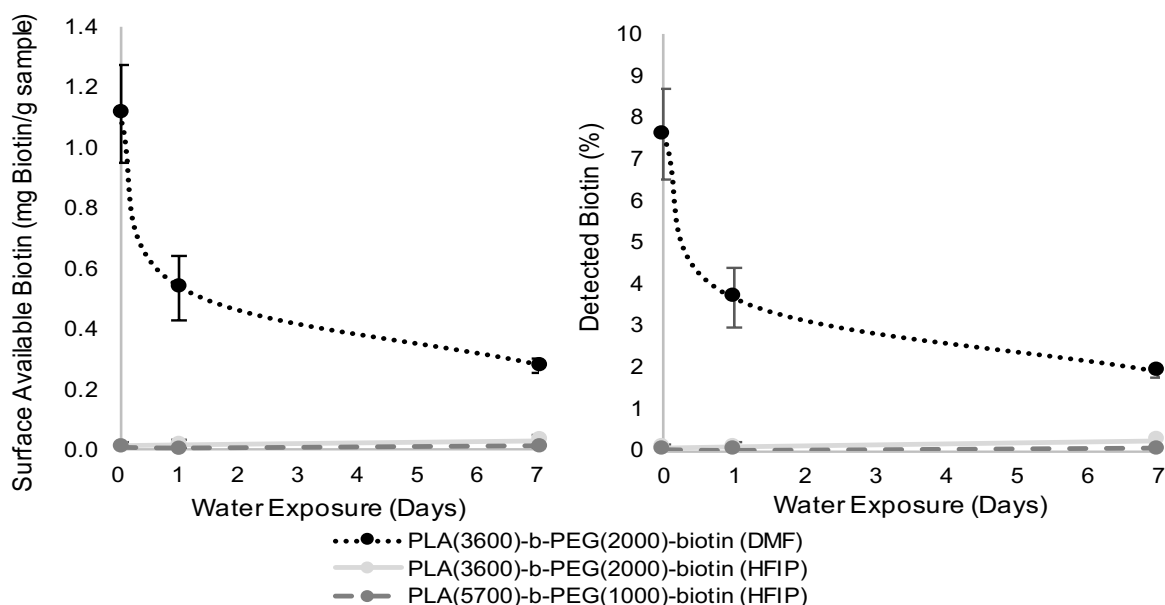


**Figure 9.** (Left) Surface available biotin and (Right) Percent biotin detected in relation to days exposed to water. Error bars represent standard error.

At this concentration, the fibers made by Li et al. were viable in biosensor devices, however, they were not studied for stability in aqueous solution. Our fibers spun from DMF with PLA(3600)-b-PEG(2000)-Biotin saw less biotin loss than that observed by Gonzalez et al., whose biotin when incorporated freely with PLA-PEG copolymers, after only one day of water exposure show no presence of biotin at the fiber's surface. With exposure to water over seven days, our fibers spun from DMF have 2 % biotin remaining at the fiber surface available for use in chemical detection.

#### 4. Conclusions

In this study we have shown tailoring the block lengths of PLA-b-PEG copolymers can lead to increased stability of electrospun fibers of PLA/PLA-b-PEG and PLA/PLA-b-PEG-Biotin in water. While HFIP dopes provided electrospun samples that were more water stable than DMF dopes, the HFIP spun samples had no biotin present at the surface of fibers for detection.



Electrospun samples of PLA(3600)-b-PEG(2000)-Biotin spun from DMF allowed for 1.1 mg of biotin per gram of fiber to be detected at the surface of fibers, with the incorporation of 85 % less biotin than previous studies.

With low hydrophilicity and no biotin detected from HFIP electrospun samples, it is necessary to continue future research with DMF as the solvent. It is still necessary to overcome the heat and organic solvent denaturing of proteins we seek to incorporate. For this reason, we intend to attach proteins to PLA3000-b- PEG2000-NHS terminals after the fibers have been electrospun from DMF.

## 5. Acknowledgements

This work was supported by the USDA National Institute of Food and Agriculture, Hatch NC1194 project #3297816. Any opinions, findings, conclusions, or recommendations expressed in this publication are those of the author(s) and do not necessarily reflect the view of the National Institute of Food and Agriculture (NIFA) or the United States Department of Agriculture(USDA). This work was also in part funded by a grant from the Department of Fiber Science & Apparel Design Graduate Student Research Awards Fund. Heating element apparatus used in electrospinning was provided by Dr. Daehwan Cho. This research made use of the Cornell Center for Materials Research Shared Facilities which are supported through the NSF MRSEC program (DMR-1120296). NSF-MRI (CHE-1531632 - PI: Aye) is acknowledged for NMR instrumentation support at Cornell University

## 6. References

1. Steyaert, I., H. Rahier, and K. De Clerck, *Nanofibre-Based Sensors for Visual and Optical Monitoring*. Electrospinning for High Performance Sensors, 2015: p. 157-177.
2. Tsou, P.H., et al., *The fabrication and testing of electrospun silica nanofiber membranes for the detection of proteins*. Nanotechnology, 2008. **19**(44).
3. Luo, Y., et al., *Surface functionalization of electrospun nanofibers for detecting E. coli O157:H7 and BVDV cells in a direct-charge transfer biosensor*. Biosensors & Bioelectronics, 2010. **26**(4): p. 1612-1617.

4. Li, D.P., M.W. Frey, and A.J. Baeumner, *Electrospun polylactic acid nanofiber membranes as substrates for biosensor assemblies*. Journal of Membrane Science, 2006. **279**(1-2): p. 354-363.
5. Hendrick, E. and M. Frey, *Increasing Surface Hydrophilicity in Poly(Lactic Acid) Electrospun Fibers by Addition of Pla-b-Peg Co-Polymers*. Journal of Engineered Fibers and Fabrics, 2014. **9**(2): p. 153-164.
6. Zhao, Y.H., et al., *Improving hydrophilicity and protein resistance of poly(vinylidene fluoride) membranes by blending with amphiphilic hyperbranched-star polymer*. Langmuir, 2007. **23**(10): p. 5779-5786.
7. Luong, N.D., et al., *Surface modification of poly(L-lactide) electrospun fibers with nanocrystal hydroxyapatite for engineered scaffold applications*. Materials Science & Engineering C-Biomimetic and Supramolecular Systems, 2008. **28**(8): p. 1242-1249.
8. Buttaro, L.M., E. Drufva, and M.W. Frey, *Phase Separation to Create Hydrophilic Yet Non-Water Soluble PLA/PLA-b-PEG Fibers via Electrospinning*. Journal of Applied Polymer Science, 2014. **131**(19).
9. Li, D., et al., *Availability of biotin incorporated in electrospun PLA fibers for streptavidin binding*. Polymer, 2007. **48**(21): p. 6340-6347.
10. Zhu, M., et al., *Streptavidin-biotin-based directional double Nanobody sandwich ELISA for clinical rapid and sensitive detection of influenza H5N1*. Journal of Translational Medicine, 2014. **12**.
11. Li, H., et al., *Construction of a biotinylated cameloid-like antibody for label-free detection of apolipoprotein B-100*. Biosensors & Bioelectronics, 2015. **64**: p. 111-118.
12. González, E., et al., *Surface Functional Poly (lactic Acid) Electrospun Nanofibers for Biosensor Applications*. Materials, 2016. **9**(1): p. 47.
13. Nuansing, W., et al., *Electrospinning of peptide and protein fibres: approaching the molecular scale*. Faraday Discussions, 2013. **166**: p. 209-221.
14. Ero-Phillips, O., M. Jenkins, and A. Stamboulis, *Tailoring Crystallinity of Electrospun Plla Fibres by Control of Electrospinning Parameters*. Polymers, 2012. **4**(3): p. 1331-1348.
15. Glotzer, S.C. and A. Coniglio, *FRUSTRATION, CONNECTIVITY, AND THE GLASS-TRANSITION*. Computational Materials Science, 1995. **4**(4): p. 325-333.

16. Tarjus, G., et al., *The frustration-based approach of supercooled liquids and the glass transition: a review and critical assessment*. Journal of Physics-Condensed Matter, 2005. **17**(50): p. R1143-R1182.
17. Kalish, J.P., et al., *Spectroscopic and thermal analyses of alpha ' and alpha crystalline forms of poly(L-lactic acid)*. Polymer, 2011. **52**(3): p. 814-821.

## 7. Supplemental Information

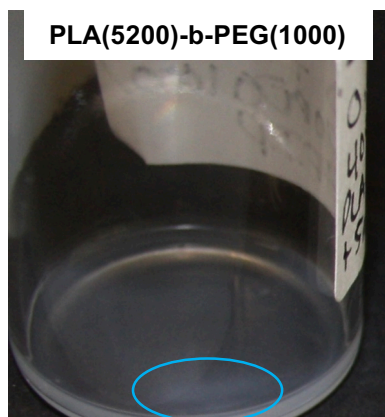


**Figure S1.** Solution of HFIP used to make 12 wt% PEG in the final fiber from PLA/PLA(5200)-b-PEG(1000). Circled is the settling of copolymer at the bottom of the vial.

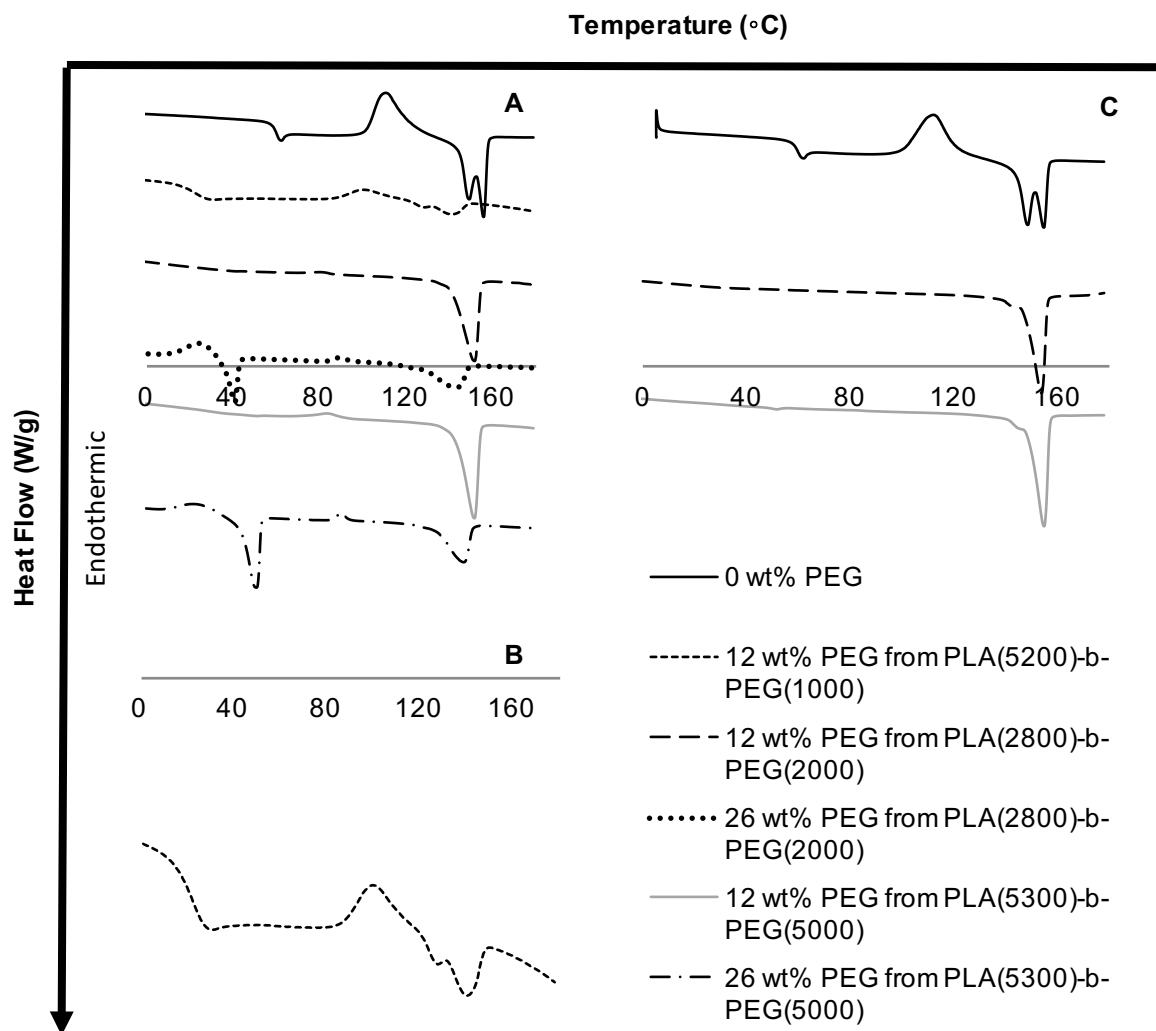


**Figure S2.** The second heating on cyclic thermographs of HFIP and DMF spun samples. (A) HFIP spun samples, (B) 12 wt% PEG from PLA(5200)-b-PEG(1000) spun from HFIP on its own graph for better visualization, and (C) DMF spun samples. Note Samples have been spaced on the graph to make them more legible. Melting temperature of PEG can be seen on the second heating for HFIP spun fibers containing 26 wt% PEG.

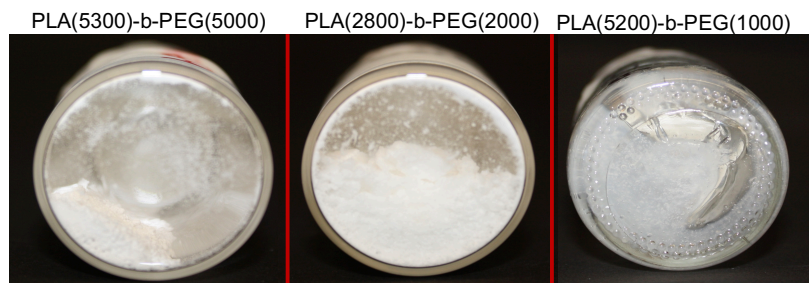


**Figure S3.** The textural appearance of PLA-b-PEG block copolymers.